Advanced Physical Research
Vol.5, No.3, 2023, pp.192-199

A STUDY OF IMPURITY DEFECT PHOTOLUMINESCENCE IN ZnSe:Cr AND ZnSe:Fe IN THE NEAR INFRARED AT ROOM TEMPERATURE

I.I. Abbasov[1*], M.A. Musayev[1], C.I. Huseynov[2], Q.Y. Eyyubov[3], N.N. Hasimova[1], A.J. Mammadova[4], A.A. Hadieva[1], Y.I. Aliyev[2,5], N.A. Qasumov[1], R.Sh. Rahimov[6]

[1]Azerbaijan State Oil and Industry University, Baku, Azerbaijan
[2]Azerbaijan State Pedagogical University, Baku, Azerbaijan
[3]Institute of Physics, Ministry of Science and Education Azerbaijan, Baku, Azerbaijan
[4]Institute of Biophysics, Ministry of Science and Education Azerbaijan, Baku, Azerbaijan
[5]Western Caspian University, Baku, Azerbaijan
[6]Baku State University, Baku, Azerbaijan

Abstract. The purpose of this work is to study the photoluminescence spectra observed ZnSe:Cr^{2+} and ZnSe:Fe^{2+} samples, is $6.1 \cdot 10^{19}$ cm^{-3} (sample 1) and $9.83 \cdot 10^{18}$ cm^{-3} (sample 3), in samples of ZnSe:Cr, and in ZnSe:Fe it is equal to $4.65 \cdot 10^{19}$ cm^{-3} (sample 2) and $7.27 \cdot 10^{18}$ cm^{-3} (sample 4) respectively. Presented a wide luminescence spectrum covering the energy range of range 0.8-1.5 μm at room temperature (T = 300 K)The samples were excited by light with a wavelength of 532nm (Nd:YAG) and 642 nm, and the luminescence spectrum showed maxima for all samples at a wavelength of 974 nm, but they differed in intensity and half-width. All broad luminescence spectra obtained during measurements were decomposed into Gaussian components. At the same time, the characteristics of the Gaussian components were determined: spectral position, i.e. λ_{max} and intensity at these maxima, half-width of maxima. The results obtained carefully analyzed.

Keywords: *ZnSe polycrystalline CVD (chemical vapor deposition), iron and chromium impurities, ZnSe:Cr and ZnSe:Fe crystals, high isostatic pressure (HIP).*

Corresponding Author: *I.I. Abbasov, Azerbaijan State Oil and Industry University, Azadlig ave., 16/21, Baku, Azerbaijan, e-mail: ibrahimabbasov179@gmail.com*

Received: *26 June 2023;* ***Accepted:*** *20 August 2023;* ***Published:*** *03 October 2023.*

1. Introduction

At present, a group of compounds is considered very promising as semiconductor materials of the near future, as evidenced, in particular, by many interesting studies of these materials (Asadullayeva *et al*., 2022; Tagiyev *et al*., 2009; Mursakulov *et al*., 2022; Abbasov *et al*., 2022; Bayramov *et al*., 2019; Mammadov *et al*., 2020; Ismayilova *et al*., 2021). This is due to the combination of the physical properties of these compounds, which make it possible to create unique devices for optics, optoelectronics, acoustoelectronics, nanoelectronics, laser technology, and the detection of ionizing radiation. At the same time, Recently, interest has increased in studying the effect of transition metals, including Cr^{2+} and Fe^{2+} ions, on the electronic structure of zinc

How to cite (APA):
I.I. Abbasov, Musayev, M.A., Huseynov, C.I.,. Eyyubov, Q.Y, Hasimova, N.N., Mammadova, A.J., …, & Rahimov, R.Sh. (2023). A study of impurity defect photoluminescence in ZnSe:Cr and ZnSe:Fe in the near infrared at room temperature. *Advanced Physical Research, 5*(3), 192-199.

chalcogenides, since they can improve the use of these materials as a working medium for broadband IR lasers, i.e. based on these ZnSe : Cr and ZnSe : Fe crystals, efficient laser generation operating at room temperature (T = 300 K) can be successfully implemented. Radiative are mainly intracenter d-d-junctions described by crystal field theory (Fedorov *et al*., 2006; Sorokina *et al*.., 2002; Mirov *et al*., 2015; Page *et al*., 1997; Balabanov *et al*., 2019; Kozlovsky *et al*., 2007; Sugano *et al*., 1970). The available works are devoted to the study of the middle infrared (IR) range, mainly at low temperatures.

In this work, we study the photoluminescence spectra observed upon excitation by semiconductor lasers (λ_{ex} = 532, 642 nm) of two chromium-doped ZnSe CVD samples and two iron-doped CVD samples in the wavelength range of 0.8–1.5 μm, i.e. in the near infrared (IR) range, at room temperature (T = 300 K). All the wide spectra obtained during the measurements were decomposed into Gaussian components and analyzed.

2. Methods and experiments

Fe and Cr film was deposited on both sides of ZnSe CVD samples by electron beam evaporation, then diffusion doping was carried out by HIP (hot isostatic pressure) treatment. Chromium and iron cations replace Zn^{2+} in the crystal lattice of zinc selenide with the Fe^{2+} and Cr^{2+} charge states neutral with respect to the lattice, and the equality of the charge states of the matrix and impurity cations contributes to a smaller deformation of the crystal lattice

The maximum concentration of chromium and iron impurities, determined by the shift of the absorption edge in the ZnSe:Cr^{2+} and ZnSe:Fe^{2+} samples, is $6.1\cdot10^{19}$ cm^{-3} (sample 1) and $9.83\cdot10^{18}$ cm^{-3} (sample 3), in samples of ZnSe:Cr, and in ZnSe:Fe it is equal to $4.65\cdot10^{19}$ cm^{-3} (sample 2) and $7.27\cdot10^{18}$ cm^{-3} (sample 4) respectively (Abbasov, 2022).

The radiation was recorded using an MS5204i monochromator spectrograph (SOL Instruments) with a diffraction grating of 1800 lines/mm and detected using an ANDOR IDUS CCD detector (model DU491A 1.7). The PL spectra were plotted after correction for the spectral sensitivity of the detecting system.

3. Results and discussion

The samples were excited by light with a wavelength of λ_{ex} = 532 and 642 nm, and the luminescence spectrum showed maxima for all samples at a wavelength of 974 nm, but they differed in intensity and half-width. In addition, as can be seen from Fig. 1,2 along with more intense and broad lines with maxima λ_{max}=974 nm, the spectra contain peaks in the wavelength range 1.26-1.3 μm with a weak intensity. In the CVD ZnSe sample doped with Cr atoms (sample 2), where the concentration of Cr atoms is lower than in the other sample (sample 1), upon excitation with light λ_{ex} = 532 and 642 nm, different spectra are observed (Fig. 1). The intensity of the maximum λ_{max} = 974 nm doped with Cr atoms (sample 2), upon excitation with light λ_{ex} = 642 nm, has the largest and minimum intensity upon excitation with light λ_{ex} = 542 nm, and for sample (sample 1) the intensity of the maximum λ_{max} = 974 nm upon excitation with light λ_{ex} = 542nm more than when excited by light λ_{ex} =642nm.

In the CVD ZnSe sample doped with Fe atoms (sample 4), where the concentration of Fe atoms is lower than in the other sample (sample 3), upon excitation with light λ_{ex} = 532 and 642 nm, different spectra are also observed (Fig. 1). The intensity of the

maximum λ_{max} = 974 nm, doped with Fe atoms (sample 4), upon excitation with light λ_{ex} = 642 nm, has the highest intensity than upon excitation with light λ_{ex} = 542 nm, and is also observed for the sample (sample 3), but the intensity of the maximum λ_{max} = 974 nm in the sample (sample 4) is greater than for the sample (sample 3).

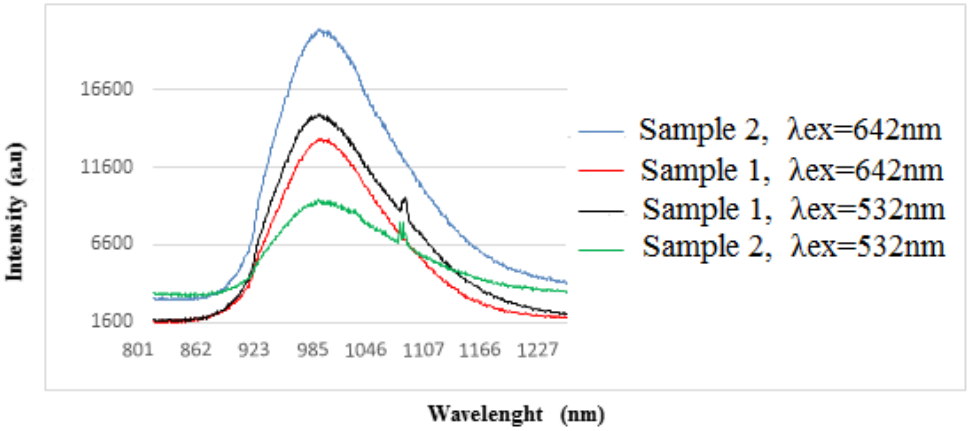

Fig. 1. PL spectra of polycrystalline CVD ZnSe: Cr^{2+} with concentration $6.1 \cdot 10^{19}$ cm^{-3} (sample 1) and $4.65 \cdot 10^{19}$ cm^{-3} (sample 2) respectively when excited by semiconductor lasers (λ_{ex} = 532, 642 nm))

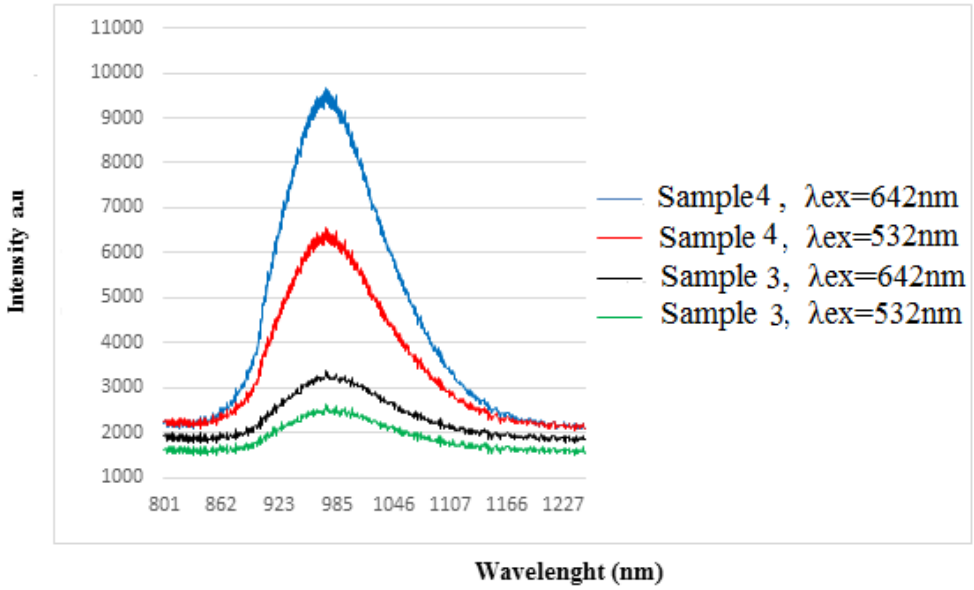

Fig. 2. PL spectra of polycrystalline CVD ZnSe: Fe^{2+} concentration $9.83 \cdot 10^{18}$ cm^{-3} (sample 3) and $7.27 \cdot 10^{18}$ cm^{-3} (sample 4) respectively when excited by semiconductor lasers (λ_{ex} = 532, 642 nm))

More intense bands with a maximum at λ_{max} = 974 nm in the ZnSe:Fe^{2+} spectra are observed upon excitation at λ_{ex} = 642 nm in a sample with a low Fe^{2+} concentration, i.e. in in ZnSe:Fe^{2+} (sample 4). And in ZnSe:Cr^{2+} samples, this is observed at a high Cr^{2+} concentration, i.e. in ZnSe:Cr^{2+} (sample 1), also upon excitation with light λ_{ex}=642 nm.

The ions of the Fe^{2+} ($3d^6$) atom and the Cr^{2+}($3d^4$) chromiums have a similar electronic configuration. It is known that the tetrahedral environment of the legends in zinc chalcogenides leads to the splitting of the ^5D singlet level of the transition metal Fe^{2+}

and Cr^{2+} due to the effect of the crystal field on doublet ^5E and triplet $^5T_2$ (Fig.3). In this case, for Fe^{2+}, the ground state is ^5E, and $^5T_2$ is the first excited state (Fig.3a), but vice versa for Cr^{2+} (Fig.3b) (Peppers *et al*., 2015).

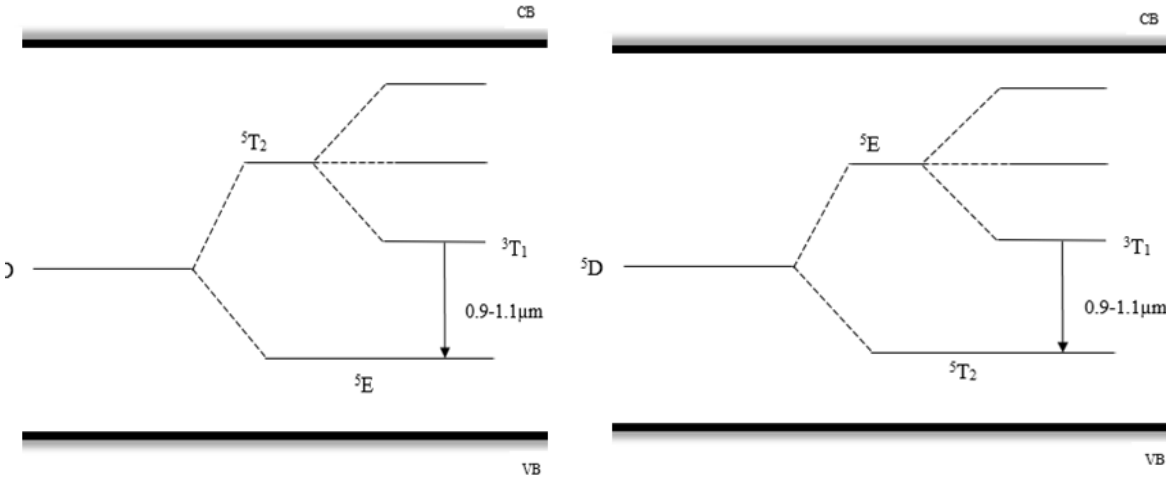

a) b)

Fig.3. Energy levels and energy transfer mechanisms of Fe^{2+} (a) and Cr^{2+} (b)

Using a light-induced electron spin study (photoexcited EPR), it was shown that the energy levels of Fe^{2+} in the band gap of ZnSe are located at a distance of 1.1 eV above the top of the valence bands, and for Cr^{2+} -1.9 eV (Surma *et al*.,1994).

Previously, the authors of (Kozlovsky et al., 2007; Sugano et al.,1970; Ushakov et al., 2021) reported that the maxima in the spectra were observed at λ_{max} = 974 nm only at nitrogen temperatures and, according to their results, this emission is associated with intracenter radiative transitions in Fe^{2+}_{Zn} centers between levels with different values of the spin $^3T_1(^3H) - {}^5E(^5D)$, which corresponds to 10267 cm^{-1}. The authors of (Kozlovsky et al.,2007; Sugano et al.,1970) also observed maxima in the wavelength range 1.26–1.3 μm at low temperatures and reported that they are associated with the $^3T_1(^3H)–{}^5T_2(^5D)$ radiative transition.

In ZnSe : Cr^{2+} samples (sample 1, 2), radiation is also associated with intracenter radiative transitions in Cr^{2+}_{Zn} centers between levels with different values of the spin $^3T_1(^3H)–{}^5T_2(^5D)$, which corresponds to 10267 cm^{-1}. And the authors of (Kozlovsky *et al*., 2007; Sugano *et al*., 1970) also observed maxima in the wavelength range of 1.26-1.3 μm at low temperatures and reported that they are associated with the radiative transition $^3T_1(^3H)–{}^5E$.

We observed these maxima at T=300K upon excitation by semiconductor lasers (λ_{ex} = 532, 642 nm), which can be taken as subgap excitation for ZnSe:Fe^{2+} and ZnSe:Cr^{2+}, since subgap excitation can lead to intracenter luminescence of iron

(Kozlovsky *et al*., 200; Sugano *et al*., 1970; Kulik *et al*., 2010). The maxima in the wavelength range 1.26-1.3 μm in the ZnSe:Cr^{2+} (sample 1) and ZnSe:Fe^{2+} (sample 4) samples upon excitation with light λ_{ex} = 642 nm are observed in a doublet form. All this shows that wide spectra in the wavelength range of 0.8–1.5 μm (Fig. 1,2) are not elementary, and therefore such complex spectra are decomposed into Gaussian components and, at the same time, the question of the structure of luminescence centers solved for each of the separated components. It is assumed that the differences in the

integrated spectra arise only due to a change in the relative contribution of the intensities of the individual components.

The decomposition of the spectra (Fig. 1,2) into Gaussian components is shown in Fig. 4, 5 and the characteristics of the components are in tables 1,2. As can be seen, the expansions of the luminescence spectrum for sample (sample 3) upon excitation λ_{ex} = 532 and 642 nm are the same, consisting of only two components, respectively, 967, 1029 nm and 968 , 1031 nm.(Fig.4a, Table 1). And for the sample (sample 4), with the same excitation, the decomposition of the spectra is also the same and consists of three components, respectively, 922,965,1018 nm and 922,967,1019 nm (Fig.4b, Table1). The amplitude and half-width of the short-wavelength component (922 nm) in both cases are small compared to the long-wavelength component. A more complicated structure of the spectrum decomposition in this case is related to the fact that the concentration of Fe atoms in this sample is low compared to sample (sample 3), which leads to an increase in the concentration of vacancies in the cationic sublattice.

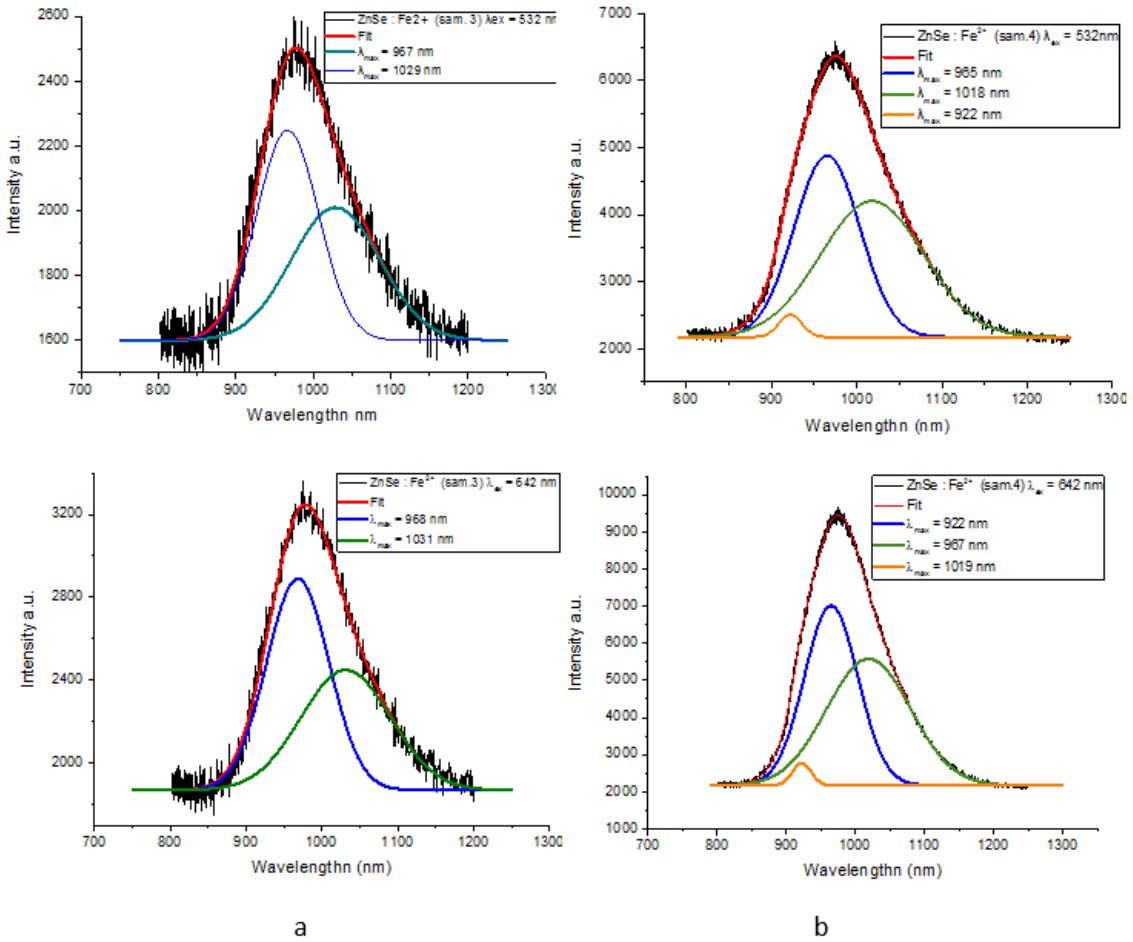

Fig. 4. Decomposition of spectra CVD ZnSe: Fe^{2+} (sample 3,4) ; Fig.2) into Gaussian components: a) sample 3, b) sample 4

For samples ZnSe : Cr^{2+} (sample 1, 2 Table 2), the decomposition of the spectra observed at the same excitation λ_{ex} = 532 and 642 nm gives very close results (Fig.5 a,b), each decomposition consisting of four component with maxima in the wavelength region: the first component in the 918– 930 nm, the second in the region of 954–969 nm, the third

in the region of 1000–1025 nm, the fourth in the region of 1090–1126 nm. Despite the weak and heavy doping of the samples ZnSe : Cr^{2+} (sample 1, 2) and excitation by various sources (λ_{ex} = 532 and 642 nm), all decompositions of the spectra for the samples ZnSe : Cr^{2+} (sample 1, 2; Fig.5) have a complex structure and, in comparison with the decomposition of the spectra for the samples ZnSe : Fe^{2+} (sample 3, 4), they exhibit long-wave mixing in the wavelength range from 1.030 to 1.126 μm. In both cases, the maximum luminescence intensity was observed at weak doping with Fe, Cr atoms, i.e. ZnSe : Fe^{2+} (sample 4) and ZnSe : Cr^{2+} (sample 2) and upon excitation with a semiconductor laser λ_{ex} = 642 nm. It is assumed that under heavy doping and with Fe and Cr atoms in CVD ZnSe, concentration quenching of luminescence occurs.

Table 1. Characteristics of Gaussian components for the luminescence spectra of samples ZnSe:Cr^{2+}(sample 1, 2)

ZnSe: Cr^{2+} nCr:$6.1\cdot10^{19}$ cm^{-3} (sample1)				ZnSe: Cr^{2+} nCr: $4.65\cdot10^{19}$ cm^{-3} (sample2)		
λ_{ex} = 532 (2.33eV)	**λ_{ex} nm (eV)**	**Maximum intensity**	**Half-with (nm)**	**λ_{ex} nm (eV)**	**Maximum intensity**	**Half-with (nm)**
	923 (1.34)	**3900**	**15**	**930(1.33)**	**4348**	**22**
	961(1.29)	**10125**	**36**	**969(1.28)**	**9653**	**36**
	1020(1.22)	**8576**	**55**	**1024(1.21)**	**6224**	**26**
	1092(1.14)	**3509**	**80**	**1093(1.13)**	**4236**	**85**
λ_{ex} = 642 (1.93eV)	**918(1.35)**	**2350**	**17**	**927(1.34)**	**5368**	**34**
	954(1.3)	**6698**	**66**	**966(01.28)**	**14285**	**72**
	1000(1.24)	**10189**	**96**	**1025(1.21)**	**11880**	**113**
	1090(1.24)	**3711**	**99**	**1026(1.1)**	**5115**	**187**

Table 2. Characteristics of Gaussian components for the luminescence spectra of amples ZnSe:Fe^{2+} (sample 3, 4)

ZnSe: Fe^{2+} nFe:$9.83\cdot10^{18}$ cm^{-3} (sample3)				ZnSe: Fe^{2+} nFe: $4.65\cdot10^{18}$ cm^{-3} (sample4)		
λ_{ex} = 532 (2.33eV)	**λ_{ex} nm (eV)**	**Maximum intensity**	**Half-with (nm)**	**λ_{ex} nm (eV)**	**Maximum intensity**	**Half-with (nm)**
	967 (1.28)	**2248**	**40**	**932(1.35)**	**2504**	**14**
		2008		**965(1.28)**	**4866**	**38**
		2890	**58**	**1018(1.22)**	**4198**	**61**
	1029(1.21)	**2445**		**922(1.35)**	**2766**	**14**
λ_{ex} = 642 (1.93eV)		**2350**	**41**		**7005**	
	968(1.28)	**6698**		**967(1.38)**	**5572**	**39**
		10189	**59**			
	1031(1.2)	**3711**		**1019(1.22)**		**61**

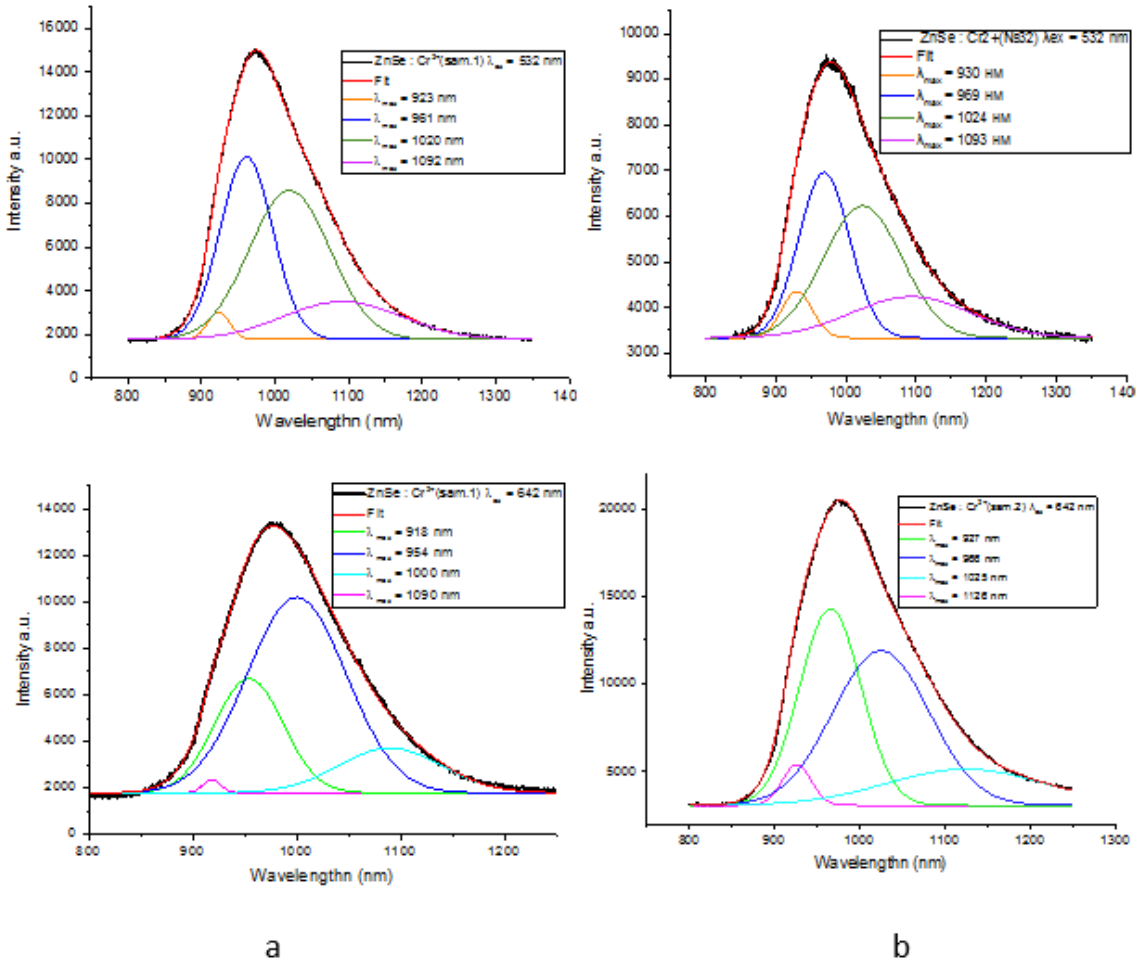

Fig. 5. Decomposition of spectra CVD ZnSe: Cr^{2+} (Sample 1, 2; Fig.1) into Gaussian components:a) sample 1, b) sample 2

4. Conclusion

For samples ZnSe:Cr^{2+} (sample 1, 2), the decomposition of the spectra, observed at the same excitation λex = 532 and 642 nm, gives very similar results (Fig. 5 a, b), and each decomposition consists of four components: t .e. have a complex structure compared to the decomposition of the spectra of samples ZnSe:Fe^{2+} (sample 3, 4), where for sample sample 3 it consists of two, and for sample 4 of three. In both cases, the maximum luminescence intensity is observed with weak doping with Fe and Cr atoms, i.e. ZnSe:Fe^{2+} (sample 4) and ZnSe: Cr^{2+} (sample 2) and when excited by a semiconductor laser λex = 642 nm. It is assumed that when heavily doped with Fe and Cr atoms in CVD-ZnSe, concentration quenching of luminescence occurs.

References

Abbasov, I., Musayev, M., Huseynov, J., Gavrishuk, E., Asadullayeva, S., Rajabli, A., & Askerov, D. (2022). Temperature behavior of X-Ray luminescence spectra of ZnSe. *International Journal of Modern Physics B, 36*(2), 2250018.

Abbasov, I.I. (2022). Study of impurities-defective luminescence in ZnSe:Cr and ZnSe:Fe in the red and near infrared range. *AJP Fizika, 28(*4), 3-6.

Asadullayeva, S.G., Ismayilova, N.A., & Eyyubov, Q.Y. (2022). Optical and electronic properties of defect chalcopyrite ZnGa2Se4: Experimental and theoretical investigations. *Solid State Communications*, 356, 11495.

Balabanov, S.S., Firsov, K.N., Gavrishchuk, E.M., Ikonnikov, V.B., Kononov, I.G, Kurashkin, S.V., Podlesnykh, S.V., Savin, D.V. & Sirotkin, A.A. (2019). Room-temperature lasing on Fe^{2+}: ZnSe with meniscus inner doped layer fabricated by solid-state diffusion bonding. *Laser Phys. Lett.*, 16055004.

Bayramov, A.I., Mamedov, N.T., Dzhafarov, T.D., Aliyeva, Y.N., Ahmadova, Kh.N., Alizade, E.H., Asadullayeva, S.Q., Sadigov, M.S., Ragimov, Sh.Kh. (2019). Photoluminescence and optical transitions in C60 fullerene thin films deposited on glass, silicon and porous silicon. *Thin Solid Films*, 690, 137566.

Fedorov, V.V., Mirov, S.B., Gallian, A., Badikov, D.V., Frolov, M.P., Korostelin, Yu.V., Kozlovsky, V.I., Landman, A.I.,. Podmarkov, Yu.P, Akimov, V.A., & Voronov, A.A. (2006). *IEEE J. Quant. Electron., 42*(9), 810-822.

Ismayilova, N.A., Abbasov, I.I. (2021). First principle calculation of electronic, optical and magnetic properties of Zn(Fe)Se compound. *International Journal of Modern Physics B, 35*(28), 2150278.

Mursakulov, N.N., Abdulzade, N.N., Jabarov, S.H., & Sabzalieva, C.E. (2022). Investigation of $CuIn_{1-x}Ga_xSe^2$ thin films for solar cells obtained by the magnetron sputtering method from two magnetrons shifted to each other. *New Materials, Compounds and Applications*, *6*(2), 140-147.

Kozlovsky, V.I., Korostelin, Yu.V., Landman, Yu.P., Podmarkov, A.I., & Frolov, M.P. (2003). Efficient lasing on a Cr2+ZnSe crystal grown from the vapor phase. *Quantum electronics, 33*(5), 408−410.

Kulik, L.L., Laiho, R., Lashkul, A.V., Lahderanta, E., Negeoglo, D.D., Negeoglo, N.D., Radevuci, I.V., Simmel, A.V., Sirkeli, V.P., & Suskevich K.D. (2010). Magnetic and luminescent properties of iron-doped ZnSe crystals. *Physica B*, 405, 4330.

Mammadov, A.I., Dang, N.T., Mehdiyeva, R.Z., Trukhanov, A.V., Asadullayeva, S.G., Trukhanov, S.V., Huseynov, R.E., & Jabarov, S.H. (2020). Structural and luminescent properties of $BaFe_{12-x}$ Al_xO_{19} compounds. *Modern Physics Letters B, 34*(35), 2050411.

Mirov, S.B., Fedorov, V.V., Martyshkin, D., Moskalev, I.S., Mirov, M., & Vasilyev, S. (2014). Progress in mid-IR lasers based on Cr and Fe-doped II–VI chalcogenides. *IEEE Journal of Selected Topics in Quantum Electronics, 21*(1), 292-310.

Page, R.H., Schaffers, K.I., DeLoach, L.D., Wilke, G.D., Patel, F.D., Tassano, J.B., Payne, S.A., Krupke, W.F., Chen, K.T., & Burger, A. (1997). Cr^{2+}- doped zinc chalcogenides as efficient, widely tunable mid-infrared lasers. *IEEE Journal of Quantum Electronics, 33*(4), 609–619.

Peppers, V.J., Fedorov, V., and Mirov, S.B. (2015). Mid-IR photoluminescence of Fe^{2+} and Cr^{2+} ions in ZnSe crystal under excitation in charge transfer bands. *Optics Express., 23*(4), 4406-4414.

Sorokina, I.T., Sorokin, E., Mirov, S.B., Fedorov, V.V., Badikov, V., Panyutin, V., & Schaffers, K., (2002). Broadly tunable compact continuous-wave Cr^{2+}:ZnS laser. *Optics Lett.,* 27, 1040.

Sugano, S., Tanabe, Y., & Kamimura, H. (1970). Multiplets of Transition-metal Ions in Crystals. N.Y. *Academic Press*, 338.

Surma, M., Godlewski, M., & Surkova, T. (1994). Iron and chromium impurities in ZnSe as centers of nonradiative recombination. *Physical Review B, 50*(12), 8319.

Tagiyev, B.G., Tagiyev, O.B., Kerimova, T.G., Guseynov, G.G., & Asadullayeva, S.G. (2009). Structural peculiarities and photoluminescence of ZnGa2Se4 compound. *Physica B: Condensed Matter*, 404, 4953-4955.

Ushakov, V.V., Aminev, D.F., Krivobok, V.S. (2021). Intracenter radiative transitions at impurity iron centers in zinc s elenide. *Fizika i Tekhnika Poluprovodnikov*, *55*(4), 304–307.